Angle-domain common-image gathers in generalized coordinates

Jeff Shragge

ABSTRACT

The theory of angle-domain common-image gathers (ADCIGs) is extended to migrations performed in generalized coordinate systems and subsurface offset axes generated by nonlinear wavefield shifts. I develop an expression linking the definition of reflection opening angle to various geometric and nonlinear shifting factors. I demonstrate that, under certain circumstances, generalized coordinate ADCIGs can be calculated directly using Fourier-based offset-to-angle approaches. Cartesian and elliptic coordinate examples are given to validate the theory. A method for eliminating geometric factors from the ADCIG expression using judicious wavefield shifts is derived; however, this approach is not likely computationally advantageous in practice.

INTRODUCTION

Angle-domain common image gathers, or ADCIGs, are used increasingly in seismic imaging to examine migration velocity model accuracy (**?**). The key idea is that migrating with correct velocity models leads to ADCIGs that do not shift vertically as a function of reflection opening angle (i.e., flat gathers). Migrating with incorrect velocity models, though, leads to inconsistent reflector depths and generates reflector smiles or frowns. ADCIGs are thus an effective analysis tool and have been incorporated in wave-equation-based inversion schemes to update velocity profiles (Sava and Biondi, 2004a,b).

ADCIGs can be generated during wave-equation imaging in a straightforward manner for both shot-profile (**?**Sava and Fomel, 2003) and shot-geophone (Prucha et al., 1999; Mosher and Foster, 2000) migration approaches. In shot-profile migration, one can generate a subsurface offset axis at each depth step by correlating the source and receiver wavefields at a number of subsurface shifts. The second step involves computing an offset-to-angle domain transformation through a post-imaging, Fourier-based stretch (Sava and Fomel, 2003).

ADCIG theory is usually developed assuming horizontal and uniformly spaced wavefield shifts, largely because wavefield extrapolation and imaging are more commonly performed in Cartesian coordinates. The introduction of shot-profile migration in non-Cartesian coordinate systems (**?**), though, warrants the development of a general ADCIG theory able to handle more arbitrary geometries and wavefield shifts.

Generalizing ADCIG theory requires properly handling the effects of non-Cartesian geometry. For example, wavefield propagation in non-Cartesian coordinate systems induces local stretches, rotations and/or shearing of the wavenumbers (**?**). Similarly, nonlinear and non-horizontal shifts can lead to angle-domain stretches.

The goal of this paper is to extend ADCIG theory to non-Cartesian geometries and nonlinear subsurface offset sampling. I demonstrate that ADCIG theory - as developed in a differential sense (Sava and Fomel, 2003) - remains valid for arbitrary geometry. Non-Cartesian coordinates do, though, introduce space-domain geometric factors that can render Fourier-based offset-to-angle methods unsuitable. I begin with a review of Cartesian ADCIG theory and provide an extension to generalized coordinate systems. I examine three canonical coordinate systems where the reflection angle can be explicitly calculated. I show how nonlinear shifting can modify the subsurface offset axis such that Fourier-based ADCIG calculation methods remain applicable.

ADCIG THEORY

The ADCIG theory presented in this section draws heavily from that presented in Sava and Fomel (2003). In the ensuing development, $\boldsymbol{x} = [x_1, x_3]$ denotes the Cartesian variables and $\boldsymbol{\xi} = [\xi_1, \xi_3]$ represents a generalized Riemannian coordinate system.

Cartesian Coordinates

For constant velocity media in Cartesian coordinates, a straightforward link exists between differential changes in the travel time, t, of rays connecting the source-reflector and reflector-receiver paths to changes in the subsurface offset, h_{x_1}, and depth, x_3, coordinates. Figure 1a shows the geometry of the variables described above. Mathematically, these relationships are expressed in the following two equations

$$\left[\begin{array}{c} \frac{\partial t}{\partial h_{x_1}} \\ \frac{\partial t}{\partial x_3} \end{array} \right] \Bigg|_{t,x_1} = 2\, s \cos\alpha \left[\begin{array}{c} \sin\gamma \\ \cos\gamma \end{array} \right], \tag{1}$$

where s is slowness, α is reflector dip, and γ is the reflection opening angle. Using the implicit functions theory, equations 1 can be rewritten as

$$\frac{\partial x_3}{\partial h_{x_1}} \Bigg|_{t,x_1} = -\frac{\partial t}{\partial h_{x_1}} \Bigg/ \frac{\partial t}{\partial x_3} = -\tan\gamma. \tag{2}$$

I introduce a negative sign in the right-hand-side of the equation above to be consistent with the notation of Sava and Fomel (2003). The left-hand side of equation 2 can be calculated in the frequency-wavenumber domain

$$\tan\gamma = -\frac{k_{h_{x_1}}}{k_{x_3}}, \tag{3}$$

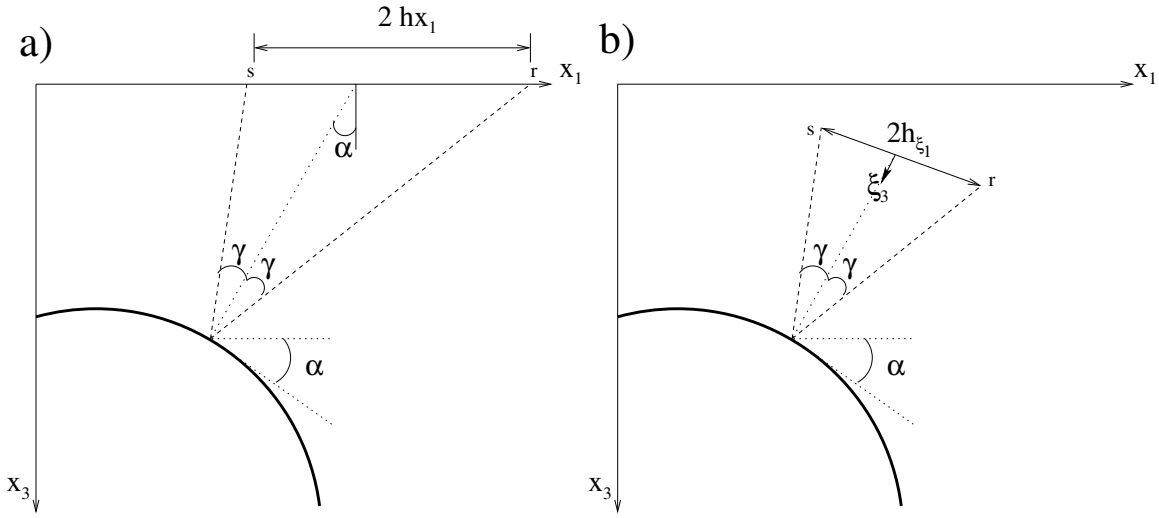

Figure 1: Zoomed in view illustrating reflection opening angle geometry. a) Cartesian coordinates. b) Generalized coordinates. Adapted from Sava and Fomel (2003). [**NR**]

where $k_{h_{x_1}}$ and k_{x_3} are the wavenumbers in the h_{x_1} and x_3 directions, respectively. Note that because equation 2 does not depend explicitly on $\boldsymbol{x}$, we may use Fourier-based methods to calculate the opening angle, γ, directly.

Generalized Coordinate Extension

Figure 1b illustrates a scenario similar to that illustrated in panel a, but for generalized coordinates. The reflection opening angle, γ, and the reflector dip, α, obviously remain unchanged; however, the orientations of the h_{ξ_1} and ξ_3 axes used to estimate γ now differ. The key question is which quantities in the ADCIG calculation are affected by this change of variables?

To answer these questions, I first assume that generalized coordinate systems are related to the Cartesian variables through a bijection (i.e., one-to-one mapping)

$$x_1 = f(\xi_1, \xi_3) \quad \text{and} \quad x_3 = g(\xi_1, \xi_3). \tag{4}$$

I also assert that the subsurface offset axes can be defined such that the implicit functions theory is valid

- h_{x_1} - a horizontal, but not necessarily linear, shift along the x_1 axis; and
- h_{ξ_1} - a shift in the direction of the ξ_1 axis commonly, though not always, sharing the same geometric qualities as the ξ_1 axis.

The bijection between the general and Cartesian coordinate systems allows us to

rewrite equations 1 as

$$\left.\begin{bmatrix} \frac{\partial t}{\partial h_{\xi_1}}\frac{\partial h_{\xi_1}}{\partial h_{x_1}} \\ \frac{\partial t}{\partial \xi_3}\frac{\partial \xi_3}{\partial x_3} \end{bmatrix}\right|_{\xi_1,t} = 2\,s\cos\alpha \begin{bmatrix} \sin\gamma \\ \cos\gamma \end{bmatrix}. \tag{5}$$

Moving partial derivatives from the left side of the equation 5 to the right yields

$$\left.\begin{bmatrix} \frac{\partial t}{\partial h_{\xi_1}} \\ \frac{\partial t}{\partial \xi_3} \end{bmatrix}\right|_{\xi_1,t} = 2\,s\cos\alpha \begin{bmatrix} \frac{\partial h_{x_1}}{\partial h_{\xi_1}}\sin\gamma \\ \frac{\partial x_3}{\partial \xi_3}\cos\gamma \end{bmatrix}. \tag{6}$$

The generalized coordinate ADCIG is given by the division by the two expressions in equation 6

$$\tan\gamma = -\left.\frac{\partial \xi_3}{\partial h_{\xi_1}}\right|_{\xi_1,t}\left[\frac{\partial x_3}{\partial \xi_3}\Big/\frac{\partial h_{x_1}}{\partial h_{\xi_1}}\right]. \tag{7}$$

The bracketed terms generally introduce a geometric dependence of the ADCIGs on coordinates $\boldsymbol{\xi}$, which can preclude the use of Fourier-based methods for calculating ADCIGs. The expression $|_{\xi_1,t}$ will be implicitly assumed for the remainder of the paper.

Defining subsurface stretch

One question arising from the geometric factors in equation 7 is what does the term $\frac{\partial h_{x_1}}{\partial h_{\xi_1}}$ represent? One way to evaluate this quantity is use a partial derivative expansion

$$\frac{\partial h_{x_1}}{\partial h_{\xi_1}} = \frac{\partial h_{x_1}}{\partial x_1}\,\frac{\partial x_1}{\partial \xi_1}\Big/\frac{\partial h_{\xi_1}}{\partial \xi_1}, \tag{8}$$

to isolate three separate terms. I interpret each contribution in the following way:

- $\frac{\partial h_{x_1}}{\partial x_1}$ - a scale factor of the transformation between h_{x_1} and x_1 usually given by $h_{x_1} = x_1$ such that $\frac{\partial h_{x_1}}{\partial x_1} = 1$;
- $\frac{\partial x_1}{\partial \xi_1}$ - the partial derivative mapping between the two coordinate systems derivable from equations 4; and
- $\frac{\partial h_{\xi_1}}{\partial \xi_1}$ a scale factor of the transformation between h_{ξ_1} and ξ_1 normally defined as $h_{\xi_1} = \xi_1$ such that $\frac{\partial h_{\xi_1}}{\partial \xi_1} = 1$, but permitted to have a parametric form $h_{\xi_1} = A(\xi_1)$.

Using the above partial derivative expansion allows us to write a general ADCIG relationship

$$\tan\gamma = -\frac{\partial \xi_3}{\partial h_{\xi_1}}\left[\left(\frac{\partial x_3}{\partial \xi_3}\frac{\partial h_{\xi_1}}{\partial \xi_1}\right)\Big/\left(\frac{\partial h_{x_1}}{\partial x_1}\frac{\partial x_1}{\partial \xi_1}\right)\right]. \tag{9}$$

In the examples below, unless stated otherwise, I assume regular sampling with linear wavefield shifting such that the following hold,

$$\begin{bmatrix} h_{x_1} \\ h_{\xi_1} \end{bmatrix} = \begin{bmatrix} x_1 \\ \xi_3 \end{bmatrix} \quad \text{or} \quad \frac{\partial h_{x_1}}{\partial x_1} = \frac{\partial h_{\xi_1}}{\partial \xi_1} = 1, \tag{10}$$

which reduces the complexity of the general coordinate ADCIG expressions to

$$\tan\gamma = -\frac{\partial \xi_3}{\partial h_{\xi_1}} \left[\frac{\partial x_3}{\partial \xi_3} \Big/ \frac{\partial x_1}{\partial \xi_1} \right]. \tag{11}$$

CANONICAL EXAMPLES

This section presents three canonical examples that illustrate the generalized ADCIG theory: Cartesian, sheared Cartesian and elliptic coordinate systems.

Cartesian Coordinates

A Cartesian coordinate system $\boldsymbol{x}$ can be defined from a unit square $\boldsymbol{\xi}$ by

$$\begin{bmatrix} x_1 \\ x_3 \end{bmatrix} = \begin{bmatrix} a & 0 \\ 0 & b \end{bmatrix} \begin{bmatrix} \xi_1 \\ \xi_3 \end{bmatrix}. \tag{12}$$

The partial differential transformation matrix is

$$\begin{bmatrix} \frac{\partial x_1}{\partial \xi_1} & \frac{\partial x_1}{\partial \xi_3} \\ \frac{\partial x_3}{\partial \xi_1} & \frac{\partial x_3}{\partial \xi_3} \end{bmatrix} = \begin{bmatrix} a & 0 \\ 0 & b \end{bmatrix}, \tag{13}$$

leading to the following differential travel-time equations

$$\begin{bmatrix} \frac{\partial t}{\partial h_{\xi_1}} \\ \frac{\partial t}{\partial \xi_3} \end{bmatrix} = 2\, s \cos\alpha \begin{bmatrix} a \sin\gamma \\ b \cos\gamma \end{bmatrix}. \tag{14}$$

The Cartesian ADCIG computation is given by

$$\tan\gamma = -\frac{b}{a} \frac{\partial \xi_3}{\partial h_{\xi_1}}. \tag{15}$$

Note that where the axes are equally sampled, one recovers the correct reflection opening angle; situations where the axes are not equally sampled require an additional scaling. This stretch is usually taken into account during the Fourier transformation implicit in equation 7.

Sheared Cartesian Coordinates

A sheared Cartesian coordinate system (see Figure 2) is an instructional, though impractical, generalized coordinate system for shot-profile migration. A sheared Cartesian mesh is defined by

$$\begin{bmatrix} x_1 \\ x_3 \end{bmatrix} = \begin{bmatrix} 1 & \sin\theta \\ 0 & \cos\theta \end{bmatrix} \begin{bmatrix} \xi_1 \\ \xi_3 \end{bmatrix}, \tag{16}$$

where θ is the shearing angle. The transformation matrix is

$$\begin{bmatrix} \frac{\partial x_1}{\partial \xi_1} & \frac{\partial x_1}{\partial \xi_3} \\ \frac{\partial x_3}{\partial \xi_1} & \frac{\partial x_3}{\partial \xi_3} \end{bmatrix} = \begin{bmatrix} 1 & \sin\theta \\ 0 & \cos\theta \end{bmatrix}, \tag{17}$$

which leads to the following differential travel-time equations

$$\begin{bmatrix} \frac{\partial t}{\partial h_{\xi_1}} \\ \frac{\partial t}{\partial \xi_3} \end{bmatrix} = 2\, s \cos\alpha \begin{bmatrix} \sin\gamma \\ \cos\theta\cos\gamma \end{bmatrix}. \tag{18}$$

The computation for ADCIGs in sheared Cartesian coordinates is

$$\tan\gamma = -\cos\theta\, \frac{\partial \xi_3}{\partial h_{\xi_1}}. \tag{19}$$

From equation 19, we can see that the apparent dips must be filtered initially by $\cos\theta$ in order to recover the true reflection opening angle.

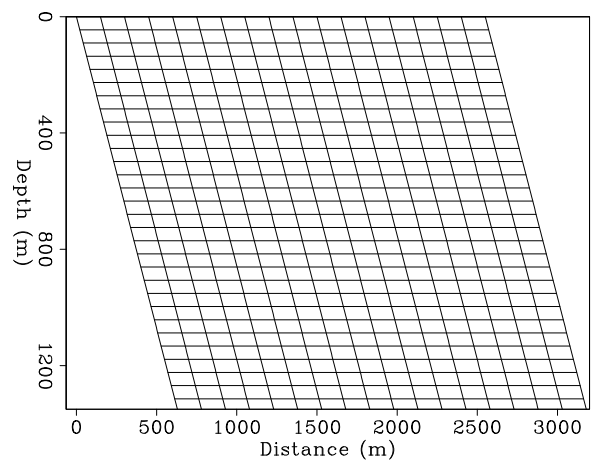

Figure 2: Example of a sheared Cartesian coordinate system with a shear angle of 25°.[**NR**]

Elliptic Coordinates

The elliptic coordinate system (see figure 3) is defined by

$$\begin{bmatrix} x_1 \\ x_3 \end{bmatrix} = \begin{bmatrix} a\cosh\xi_3\cos\xi_1 \\ a\sinh\xi_3\sin\xi_1 \end{bmatrix}. \tag{20}$$

The transformation matrix is defined by

$$\begin{bmatrix} \frac{\partial x_1}{\partial \xi_1} & \frac{\partial x_1}{\partial \xi_3} \\ \frac{\partial x_3}{\partial \xi_1} & \frac{\partial x_3}{\partial \xi_3} \end{bmatrix} = a \begin{bmatrix} \cosh \xi_3 \sin \xi_1 & \sinh \xi_3 \cos \xi_1 \\ -\sinh \xi_3 \cos \xi_1 & \cosh \xi_3 \sin \xi_1 \end{bmatrix}, \tag{21}$$

which leads to the following differential travel-time equations

$$\begin{bmatrix} \frac{\partial t}{\partial h_{\xi_1}} \\ \frac{\partial t}{\partial \xi_3} \end{bmatrix} = 2\, s \cos\alpha \begin{bmatrix} \sin \gamma \left(a \cosh \xi_3 \sin \xi_1 \right) \\ \cos \gamma \left(a \cosh \xi_3 \sin \xi_1 \right) \end{bmatrix}. \tag{22}$$

The computation for the ADCIG in elliptic coordinates is given by

$$\tan \gamma = -\frac{\partial \xi_3}{\partial h_{\xi_1}}. \tag{23}$$

Thus, ADCIGs calculated in elliptic coordinates directly yield the reflection opening angle without any additional filtering.

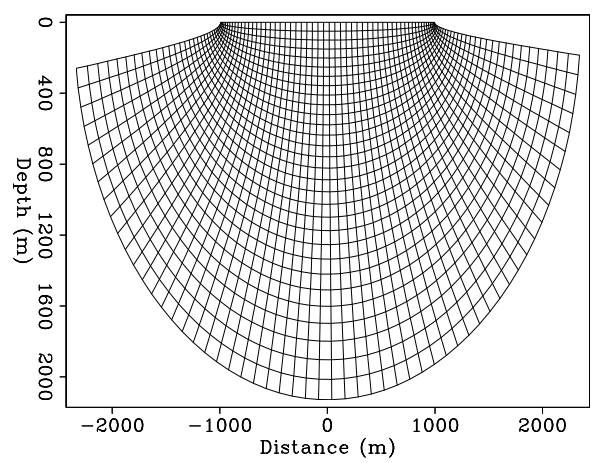

Figure 3: Example of an elliptic coordinate system. [**NR**]

NUMERICAL EXAMPLES

This section presents a numerical test of the generalized theory by comparing ADCIGs from Cartesian and elliptic coordinate systems for the BP synthetic velocity model. **?** demonstrate that the elliptic coordinate system does not induce an anisotropic wavenumber stretch during wavefield extrapolation. I assert that equation 23 is a similar expression, and is a further argument that the Cartesian and elliptic coordinate ADCIGs should yield similar results. (The results are not necessarily equal due to the differing wavefield extrapolation accuracy.)

The numerical examples presented herein were generated using a shot-profile migration algorithm with extrapolation operators accurate to roughly 80° (Lee and Suh, 1985). For each profile I did the following: i) computed 31 subsurface shifts at each extrapolation step; ii) calculated ADCIGs using the procedure described in Sava and

Fomel (2003); and iii) interpolated the single-shot ADCIG output to the global image volume.

The top and bottom panels of figure 4 show the image volumes for the elliptic and Cartesian coordinate systems, respectively. I indicate a number of locations where the elliptic coordinate system produces superior images. Figure 5 shows the ADCIGs

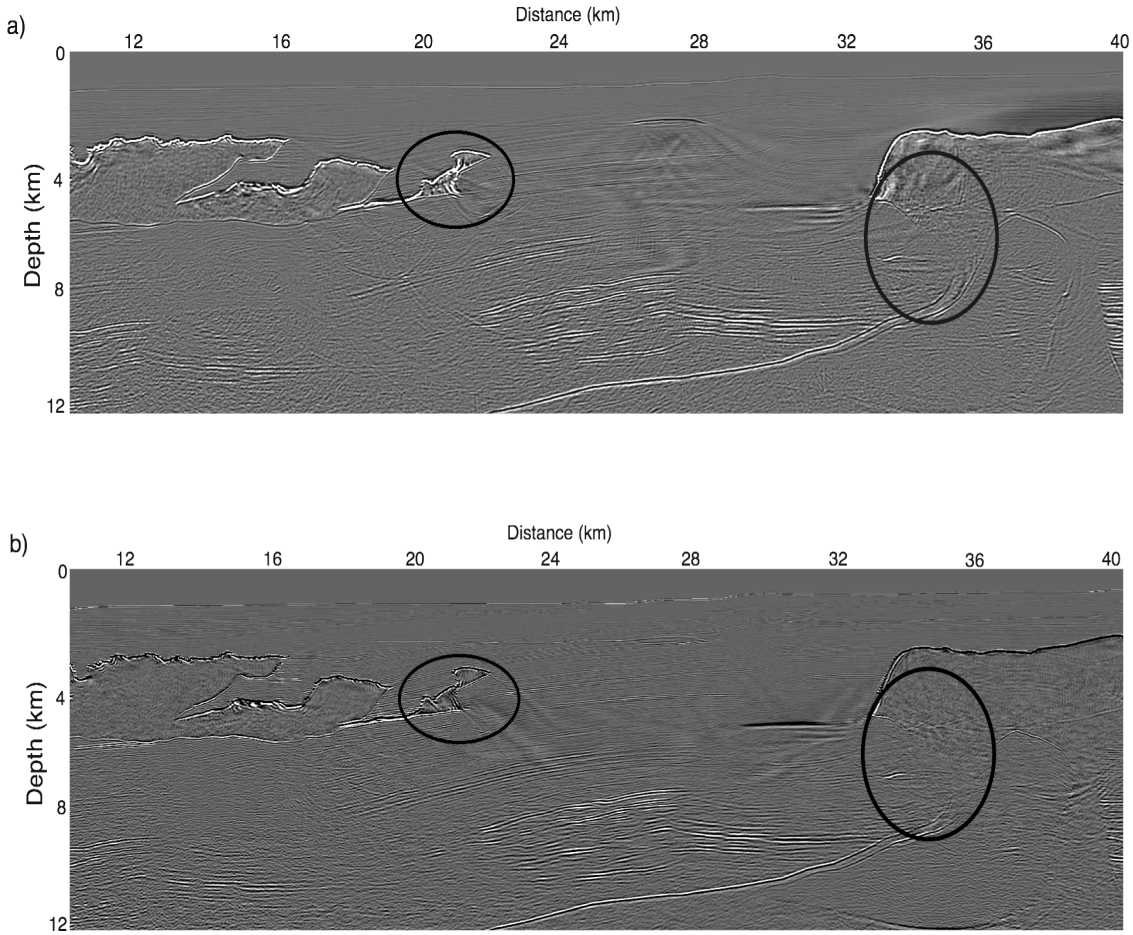

Figure 4: Comparative BP velocity model images for the elliptic (top panel) and Cartesian (bottom panel) coordinate systems.[**CR**]

corresponding to figure 4 for the elliptic (top panel) and Cartesian (bottom panel) coordinate systems. The ADCIGs are spaced out every 500 meters, and have an angular bandwidth of $[-60^\circ < \gamma < 60^\circ]$. Note that the ADCIGs are flat, though with slightly different amplitudes caused by differing illumination. The similarity between these gathers indicates the validity of the general coordinate ADCIG theory.

A second test that illustrates the validity of this approach is to examine how the ADCIGs change when the velocity profile is altered. For this test, we rescale the BP synthetic velocity profile by factors from 0.92x to 1.08x in increments of 0.02x and migrate a single shot-profile. Figure 6 presents the elliptic coordinate ADCIG results

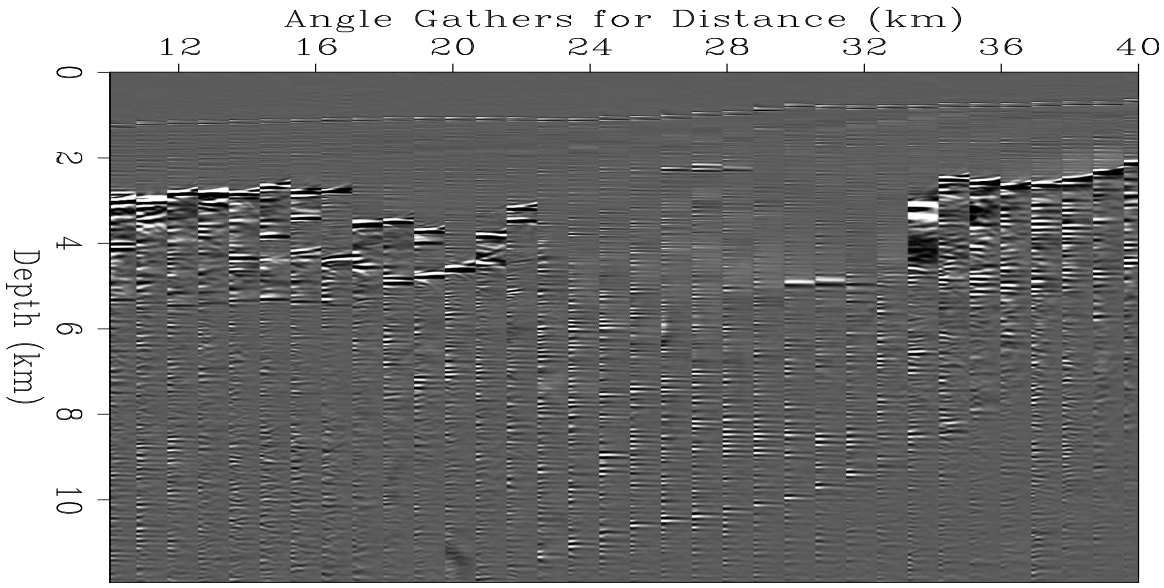

Figure 5: ADCIGs corresponding to the images in figure 4 calculated in the elliptic coordinates.[**CR**]

for an ADCIG and shot point coincidentally located at 12000 m. As we progress from the leftmost (too slow) to the rightmost (too fast) panels, we observe that the imaged reflections go from smiling to frowning. As expected, the ADCIG is most flat and well-focused where the true velocity model is used.

ELIMINATING SPATIAL DEPENDENCY

This section presents a method for eliminating the spatial dependency of generalized ADCIG transforms through a judicious stretching of the subsurface offset axis. Revisiting how one can introduce a stretch using equation 11, one obvious restriction to make is maintaining uniform Cartesian spatial sampling. I accomplish this by enforcing $\frac{\partial h_{x_1}}{\partial x_1} = 1$ such that

$$\tan\gamma = -\frac{\partial \xi_3}{\partial h_{\xi_1}} \left[\frac{\partial h_{\xi_1}}{\partial \xi_1} \frac{\partial x_3}{\partial \xi_3} \Big/ \frac{\partial x_1}{\partial \xi_1} \right]. \tag{24}$$

The next step is to specify the relationship between h_{ξ_1} and ξ_1 that enables us to calculate $\frac{\partial h_{\xi_1}}{\partial \xi_1}$. One useful *ansatz* solution is

$$\frac{\partial h_{\xi_1}}{\partial \xi_1} = \frac{\partial x_1}{\partial \xi_1} \Big/ \frac{\partial x_3}{\partial \xi_3}. \tag{25}$$

Substituting equation 25 into equation 24 generates the following ADCIG

$$\tan\gamma = -\frac{\partial \xi_3}{\partial h_{\xi_1}}. \tag{26}$$

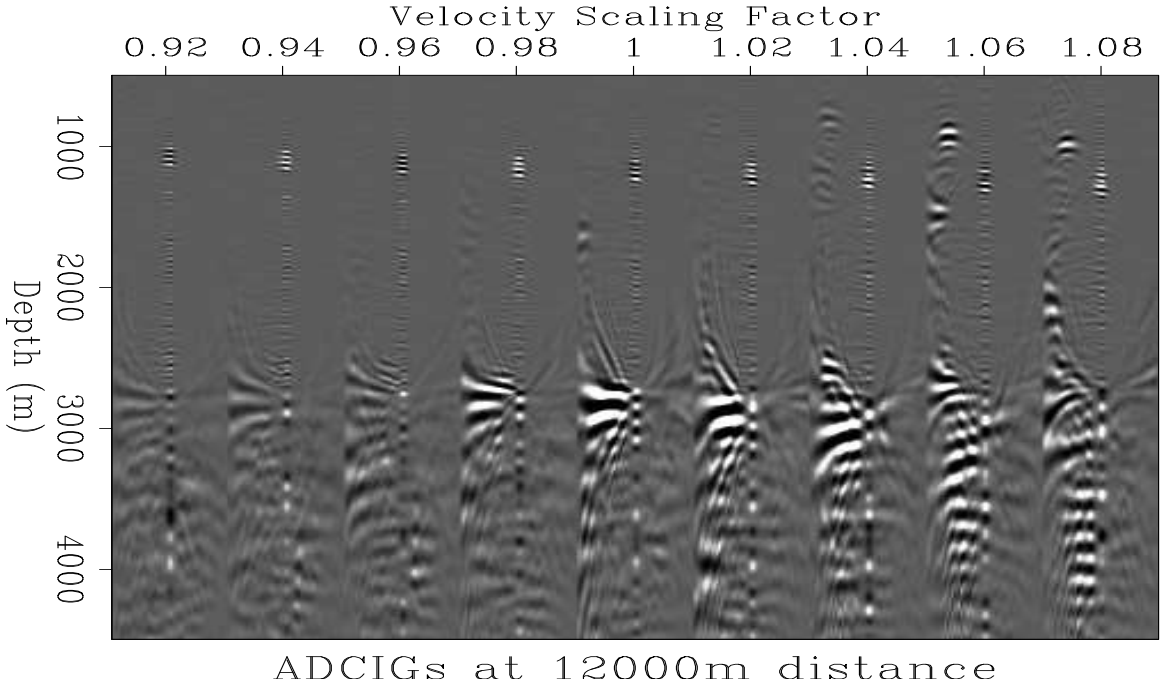

Figure 6: Single shot-profile migration ADCIGs for a coincident ADCIG and source point at 12000 m. Note that the image is best focused when the correct velocity is used, and frowns and smiles are observed when migration velocity is used. [**ER**]

Equation 25 implies that if we can define an appropriate coordinate system stretch for each $\boldsymbol{\xi}$ location, we may still recover the reflection opening angle using Fourier-based techniques.

Polar coordinate example

The polar coordinate system, where the extrapolation direction is oriented in the angular rather than the radial direction (see figure 7), is defined by

$$\begin{bmatrix} x_1 \\ x_3 \end{bmatrix} = \begin{bmatrix} a\,\xi_1 \cos\xi_3 \\ a\,\xi_1 \sin\xi_3 \end{bmatrix}. \tag{27}$$

The partial derivative transformation matrix between the two systems is

$$\begin{bmatrix} \frac{\partial x_1}{\partial \xi_1} & \frac{\partial x_1}{\partial \xi_3} \\ \frac{\partial x_3}{\partial \xi_1} & \frac{\partial x_3}{\partial \xi_3} \end{bmatrix} = \begin{bmatrix} a\cos\xi_3 & -a\,\xi_1 \sin\xi_3 \\ a\sin\xi_3 & a\,\xi_1\cos\xi_3 \end{bmatrix}, \tag{28}$$

leading to the following differential travel-time equations

$$\begin{bmatrix} \frac{\partial t}{\partial h_{\xi_1}} \\ \frac{\partial t}{\partial \xi_3} \end{bmatrix} = 2\,s\cos\alpha \begin{bmatrix} a\cos\xi_3 \sin\gamma \\ a\,\xi_1 \cos\xi_3 \cos\gamma \end{bmatrix}. \tag{29}$$

Inserting equations 28 into equation 24 generates the expression for polar coordinate ADCIGs

$$\tan\gamma = \frac{\partial \xi_3}{\partial h_{\xi_1}} \left[\xi_1 \frac{\partial h_{\xi_1}}{\partial \xi_1} \right]. \tag{30}$$

Thus, one cannot calculate ADCIGs directly in a polar coordinate system unless the spatial dependency is judiciously eliminated.

The polar coordinate system provides an example where ADCIGs contain a geometric dependence on $\boldsymbol{\xi}$. Inserting the geometric factors $\frac{\partial x_1}{\partial \xi_1}$ and $\frac{\partial x_3}{\partial \xi_3}$ from above into equation 25 leads to

$$\frac{\partial h_{\xi_1}}{\partial \xi_1} = \frac{\partial x_1}{\partial \xi_1} \Big/ \frac{\partial x_3}{\partial \xi_3} = \frac{1}{\xi_1}. \tag{31}$$

Integrating along surfaces of constant ξ_3 yields

$$h_{\xi_1} = \ln \xi_1. \tag{32}$$

Equation 32 defines the subsurface axis stretch required to directly calculate ADCIGs by Fourier-based approaches.

One question is how best to perform this stretch. One approach would be to perform linear shifting and then regrid that result to an natural log grid. However, the computational overhead renders this method less-than-ideal, especially for situations where estimating $\frac{\partial h_{\xi_1}}{\partial x_3}$ directly by slant-stack processing is more efficient. However, this remains an open research topic.

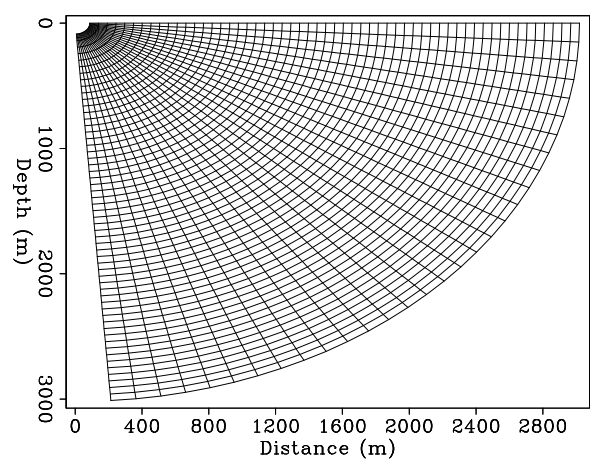

Figure 7: Example of a polar coordinate system. [**NR**]

CONCLUSIONS

This paper extends the Cartesian ADCIG theory to generalized coordinate systems. The expressions for ADCIGs contain additional coordinate factors describing mesh geometry and wavefield shifts. The method for calculating ADCIGs in an elliptic coordinate system is identical to a Cartesian ADCIG calculation as confirmed by

numerical examples. An approach for eliminating the spatial dependency is given; however, this approach is not likely efficient in practice and slant stack calculations will be used an as alternative.

ACKNOWLEDGMENTS

I would like to thank Alejandro Valenciano for helpful discussions, and BP for releasing the synthetic data used in the examples.

REFERENCES

Lee, M. W. and S. Y. Suh, 1985, Optimization of one-way wave-equations (short note): Geophysics, **50**, 1634–1637.

Mosher, C. and D. Foster, 2000, Common angle imaging conditions for prestack depth migration: 70th Ann. Internat. Mtg, 830–833, Soc. of Expl. Geophys.

Prucha, M., B. Biondi, and W. Symes, 1999, Angle-domain common image gathers by wave-equation migration: 69th Ann. Internat. Mtg, 824–827, Soc. of Expl. Geophys.

Sava, P. and B. Biondi, 2004a, Wave-equation migration velocity analysis. I. Theory: Geophys. Prosp., **52**, 593–606.

———, 2004b, Wave-equation migration velocity analysis. Ii. Subsalt imaging examples: Geophys. Prosp., **52**, 607–623.

Sava, P. C. and S. Fomel, 2003, Angle-domain common-image gathers by wavefield continuation methods: Geophysics, **68**, 1065–1074.